RADC-TR-83-286
In-House Report
December 1983

THE EFFECTS OF A LOW-ALTITUDE NUCLEAR BURST ON MILLIMETER WAVE PROPAGATION

Edward E. Altshuler

ROME AIR DEVELOPMENT CENTER
Air Force Systems Command
Griffiss Air Force Base, NY 13441

This report has been reviewed by the RADC Public Affairs Office (PA) and is releasable to the National Technical Information Service (NTIS). At NTIS it will be releasable to the general public, including foreign nations.

RADC-TR-83-286 has been reviewed and is approved for publication.

APPROVED: John E Rasmussen

JOHN E. RASMUSSEN
Chief, Propagation Branch
Electromagnetic Sciences Division

APPROVED: Allan C Schell

ALLAN C. SCHELL
Chief, Electromagnetic Sciences Division

Accession For	
NTIS GRA&I	X
DTIC TAB	☐
Unannounced	☐
Justification	
By	
Distribution/	
Availability Codes	
Dist	Avail and/or Special
A/1	

FOR THE COMMANDER: John A. Ritz

JOHN A. RITZ
Acting Chief, Plans Office

If your address has changed or if you wish to be removed from the RADC mailing list, or if the addressee is no longer employed by your organization, please notify RADC (EEPS) Hanscom AFB MA 01731. This will assist us in maintaining a current mailing list.

Do not return copies of this report unless contractual obligations or notices on a specific document requires that it be returned.

Unclassified

SECURITY CLASSIFICATION OF THIS PAGE

REPORT DOCUMENTATION PAGE

1a. REPORT SECURITY CLASSIFICATION: Unclassified	1b. RESTRICTIVE MARKINGS
2a. SECURITY CLASSIFICATION AUTHORITY	3. DISTRIBUTION/AVAILABILITY OF REPORT: Approved for public release; distribution unlimited.
2b. DECLASSIFICATION/DOWNGRADING SCHEDULE: N/A	
4. PERFORMING ORGANIZATION REPORT NUMBER(S): RADC-TR-83-286	5. MONITORING ORGANIZATION REPORT NUMBER(S)
6a. NAME OF PERFORMING ORGANIZATION: Rome Air Development Center; 6b. OFFICE SYMBOL (If applicable): (EEPS)	7a. NAME OF MONITORING ORGANIZATION
6c. ADDRESS (City, State and ZIP Code): Hanscom AFB, Massachusetts 01731	7b. ADDRESS (City, State and ZIP Code)
8a. NAME OF FUNDING/SPONSORING ORGANIZATION; 8b. OFFICE SYMBOL (If applicable)	9. PROCUREMENT INSTRUMENT IDENTIFICATION NUMBER
8c. ADDRESS (City, State and ZIP Code)	10. SOURCE OF FUNDING NOS.

PROGRAM ELEMENT NO.	PROJECT NO.	TASK NO.	WORK UNIT NO.
62702F	4600	16	07

11. TITLE (Include Security Classification): The Effects of a Low-Altitude Nuclear Burst on (Contd)

12. PERSONAL AUTHOR(S): Edward E. Altshuler

13a. TYPE OF REPORT	13b. TIME COVERED	14. DATE OF REPORT (Yr., Mo., Day)	15. PAGE COUNT
	FROM _____ TO _____	1983 December	23

16. SUPPLEMENTARY NOTATION: RADC Project Engineer: Edward E. Altshuler, RADC/EEPS

17. COSATI CODES			18. SUBJECT TERMS (Continue on reverse if necessary and identify by block number)
FIELD	GROUP	SUB. GR.	Dust attenuation; Millimeter wavelengths; Nuclear burst dust

19. ABSTRACT (Continue on reverse if necessary and identify by block number)

~~The main objective of~~ this report ~~is to~~ examines the limitations imposed on mm ~~millimeter~~ wave propagation by the dust produced by a low altitude nuclear burst. The closer the burst is to the surface, the larger will be the dust loaded into the nuclear fireball, an extremely hot and highly ionized spherical mass of air and gaseous weapons residues. The fireball absorbs, scatters and refracts the propagated wave and may also produce scintillations. In this study, only losses due to absorption and scattering are calculated.

Since there is a great deal of uncertainty as to how representative the dust model is of the true nuclear environment, a sensitivity analysis of attenuation dependence of the pertinent dust parameters was first conducted. It was found that the dust attenuation is ~~very~~ heavily dependent on the maximum particle radius, the number of large particles in the distribution and the real and imaginary components of the index of refraction over the range from dry sand to clay. (Contd)

20. DISTRIBUTION/AVAILABILITY OF ABSTRACT	21. ABSTRACT SECURITY CLASSIFICATION
UNCLASSIFIED/UNLIMITED ☐ SAME AS RPT. ☒ OTIC USERS ☐	Unclassified

22a. NAME OF RESPONSIBLE INDIVIDUAL	22b. TELEPHONE NUMBER (Include Area Code)	22c. OFFICE SYMBOL
Edward E. Altshuler	617-861-4662	EEPS

DD FORM 1473, 83 APR EDITION OF 1 JAN 73 IS OBSOLETE.

Unclassified

SECURITY CLASSIFICATION OF THIS PAGE

11. Contd

Millimeter Wave Propagation

---

19. Contd)

The attenuation is also proportional to the fraction of the atmosphere filled with dust. The total attenuation produced by a 1 megaton burst at the surface is then computed using the WESCOM code. The attenuation includes losses due to fireball ionization, dust and atmospheric oxygen and water vapor. Results are obtained as a function of time after burst, distance from burst, elevation angle and frequency up to 95 GHz. It is found that very high attenuations occur within about 20 sec after the burst if the path intersects the fireball. At later times attenuations of the order of tens of dB are possible due to dust alone. After several minutes the larger dust particles have settled and attenuations of several dB are present. Oxygen and water vapor attenuations are typically less than 1 dB in the window regions.

Contents

Illustrations

Tables

The Effects of a Low-Altitude Nuclear Burst on Millimeter Wave Propagation

I. INTRODUCTION

In this report the limitations imposed on millimeter waves by a low altitude nuclear burst are examined. Associated with the burst is a fireball, an extremely hot and highly ionized spherical mass of air and gaseous weapon residues. The fireball grows rapidly and because of its intense heat some of the soil and other material in the area are vaporized and taken into the fireball; strong afterwinds cause large amounts of dirt and debris to be sucked up as the fireball rises.

In order to estimate the effects of dust on the performance of a millimeter wave system it is necessary to first develop a dust model. Since there is a great deal of uncertainty as to how representative the model is of the true nuclear environment, a sensitivity analysis of the attenuation dependence on pertinent dust parameters is conducted. It is assumed that the dust particle sizes follow a power law distribution. Then the attenuation is computed as a function of minimum particle radius, maximum particle radius, particle size distribution, index of refraction and density. A Mie formulation is used to calculate the absorption and scattering losses produced by dust.

The total attenuation produced by a 1 Megaton surface burst is then computed using the WESCOM code. The attenuation consists of contributions due to fireball

(Received for publication 1 February 1985)

ionization, dust and atmospheric oxygen and water vapor. Attenuations are obtained as a function of time after burst, distance from burst, elevation angle and frequency.

2. PARTICLE SIZE DISTRIBUTION

The sizes of dust particles are often represented by a power law probability distribution of the form

$$P(r) = kr^{-p} \tag{1}$$

where r is the particle radius, p is the exponent and k is a constant, selected such that P(r) is a proper probability distribution. For some applications a log-normal distribution of particle sizes is used since it provides a better model of the very small particles. For this study, however, we will show that the actual distribution of the very small dust particles does not significantly affect the attenuation so the power law distribution is suitable.

Thus

$$k \int_{r_{min}}^{r_{max}} r^{-p}\, dr = 1 . \tag{2}$$

Solving for k we have

$$k = \frac{p-1}{r_{min}^{-(p-1)} - r_{max}^{-(p-1)}} \tag{3}$$

where r_{min} and r_{max} are the minimum and maximum particle radii respectively. The total number of particles of radius r is then

$$N(r) = N_T P(r) \tag{4}$$

where N_T is the total number of dust particles,

$$N_T = \frac{M_T}{\rho_b \overline{V}} \tag{5}$$

and

M_T = total mass of particulates,

ρ_b = bulk density of particulate material,

$\overline{V}$ = mean volume of a particulate.

Then

$$N(r) = \frac{M_T}{\rho_b (4/3\,\pi r^3)} \cdot \frac{p-1}{r_{min}^{-(p-1)} - r_{max}^{-(p-1)}}\, r^{-p} . \tag{6}$$

It can be shown that

$$r^3 = \frac{p-1}{p-4} \cdot \frac{r_{min}^{-(p-4)} - r_{max}^{-(p-4)}}{r_{min}^{-(p-1)} - r_{max}^{-(p-1)}} .$$

Finally,

$$N(r) = \frac{M_T\,(p-4)\,r^{-p}}{4/3\,\pi\,\rho_b \left[r_{min}^{-(p-4)} - r_{max}^{-(p-4)}\right]} . \tag{8}$$

3. ATTENUATION OF DUST PARTICLES

Millimeter waves incident on atmospheric particulates undergo absorption and scattering, the degree of each being dependent on the size, shape and complex dielectric constant of the particle and the wavelength and polarization of the wave. An expression for calculating the absorption and scattering from a dielectric sphere was first derived by Mie.[1] It has the form

$$Q_t = -\frac{\lambda^2}{2\pi}\, \mathrm{Re} \sum_{n=1}^{\infty} (2n+1)\,(a_n^s + b_n^s) \tag{9}$$

1. Mie, G. (1908) Contribution to the optics of suspended media specifically colloial metal suspensions (in German), Ann. Physik, 25:377-445.

where Q_t, the extinction cross section, represents losses due to both absorption Q_a, and scattering Q_s, and a_n^s and b_n^s are very complicated functions of the spherical Bessel terms that correspond to the magnetic and electric modes of the particle respectively. Q_t has the dimension of area and is usually expressed as cm^2. Physically, if a wave having a flux density of S W/cm^2 is incident on the particle, then $S \times Q_t$ is the power absorbed and scattered.

When the size of a dust particle is very small with respect to wavelength, then the Rayleigh approximation is valid. For this case

$$Q_a = \frac{8\pi^2 r^3}{\lambda} \operatorname{Im}\left(-\frac{n^2-1}{n^2+2}\right) \tag{10}$$

$$Q_s = \frac{128\pi^5 r^6}{3\lambda^4} \left|\frac{n^2-1}{n^2+2}\right|^2 . \tag{11}$$

It is seen that the absorption is inversely proportional to the wavelength while the scattering loss is inversely proportional to the fourth power of the wavelength; thus when the wavelength is large compared to the particle size, the absorption dominates and scattering losses are often assumed negligible. Furthermore, since the absorption is proportional to the particle volume, the total attenuation is proportional to the total volume of dust.

As the dust particles become larger, then the Rayleigh approximation is no longer valid and the Mie formulation must be used. Both absorption and scattering cross sections continue to increase with particle size. Finally, after reaching a peak the total cross section begins to level off and would eventually approach a value of twice the geometric cross section of the particle when it is very large with respect to wavelength.[2] Thus we note that as the particle becomes larger the extinction cross section which was initially proportional to the particle volume becomes proportional to the particle cross sectional area.

The attenuation coefficient is equal to

$$\alpha = \int_0^\infty N(r)\, Q_t\, dr . \tag{12}$$

This expression is in nepers/cm; if r and Q_t have units of cm and N(r) is in cm^{-3}. In order to convert to dB/km a multiplicative factor of 4.343×10^5 must be introduced.

---

2. Van De Hulst, H. C. (1957) Light Scattering by Small Particles, Wiley, New York.

Attenuation and albedo, the ratio of scattered loss to total loss $\frac{Q_s}{Q_t}$, for a particle size power law distribution are plotted in Figure 1 for sand and clay for frequencies from 10 to 95 GHz. It is assumed that the minimum and maximum particle radii are 0.005 and 5 mm respectively, that the power law exponent is -3.5, and that the densities of the dust material and average mass are 2.6 gm/cm^3 and 100 gm/m^3 respectively. It is seen that the attenuation increases very rapidly with increasing frequency. It should be pointed out that attenuation is plotted on a logarithmic scale so the apparent linear increase in attenuation at the higher frequencies actually corresponds to an exponential increase, in reality. Since clay has a higher index refraction than sand, the attenuations are significantly higher.

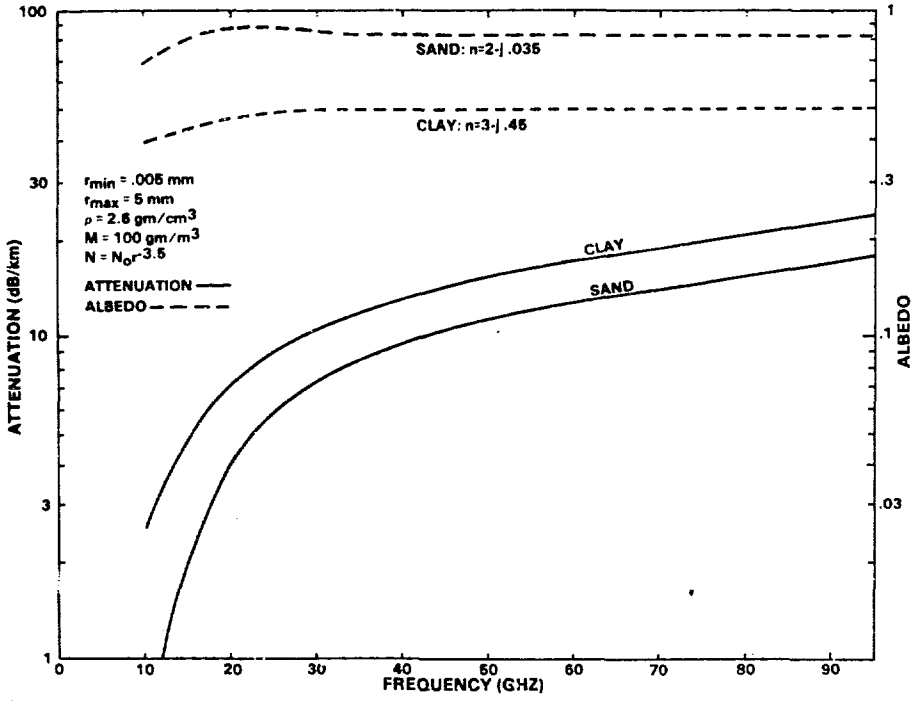

Figure 1. Attenuation and Albedo of Sand and Clay Particles at Millimeter Wavelengths

The ratio of the scattering losses to the total losses, often referred to as the albedo, is also plotted in Figure 1. It is interesting to note that the albedo for sand is approximately 0.7, even for a wavelength as long as 30 mm when the average particle radius is only 0.02675 mm, less than 0.001 wavelength. This indicates that even though the average dust particles are very small with respect to

wavelength the scattering losses are certainly not negligible as compared to the absorption because of the limited number of large particles that are present. This issue is discussed later when the results of the albedo dependence on maximum particle radius are presented.

3.1 Dependence of Dust Attenuation on Minimum Particle Radius

In Figures 2a and 2b, the attenuations are plotted for sand and clay respectively as a function of minimum particle radius for a set of frequencies from 10 to 95 GHz. It is seen that the attenuation rises only very slightly as the minimum particle radius is increased. It is interesting to note that it passes through a very broad peak at 95 GHz and would probably behave similarly at the lower frequencies for larger minimum particle radii. On the basis of these results it can be concluded that the attenuation is not very sensitive to the minimum particle radius.

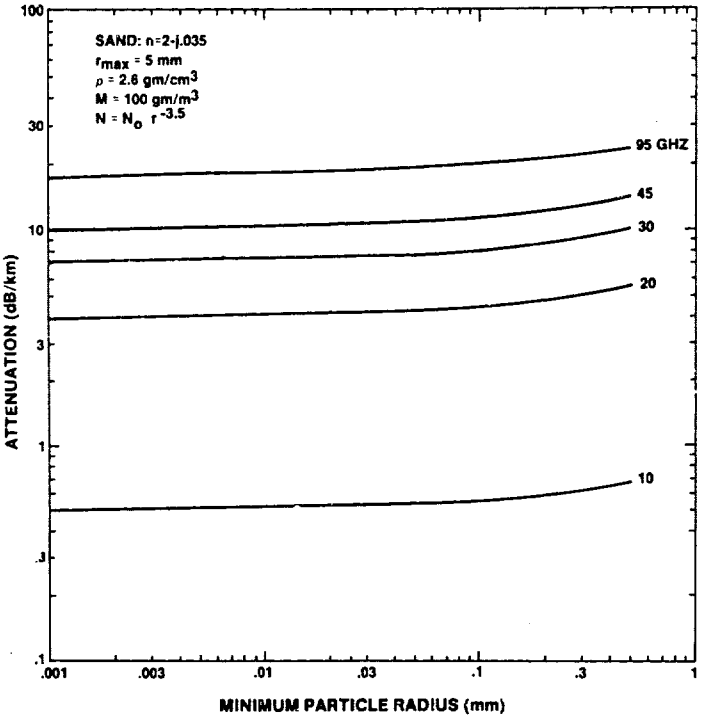

Figure 2a. Attenuation at Millimeter Wavelengths as a Function of Minimum Particle Radius, Sand

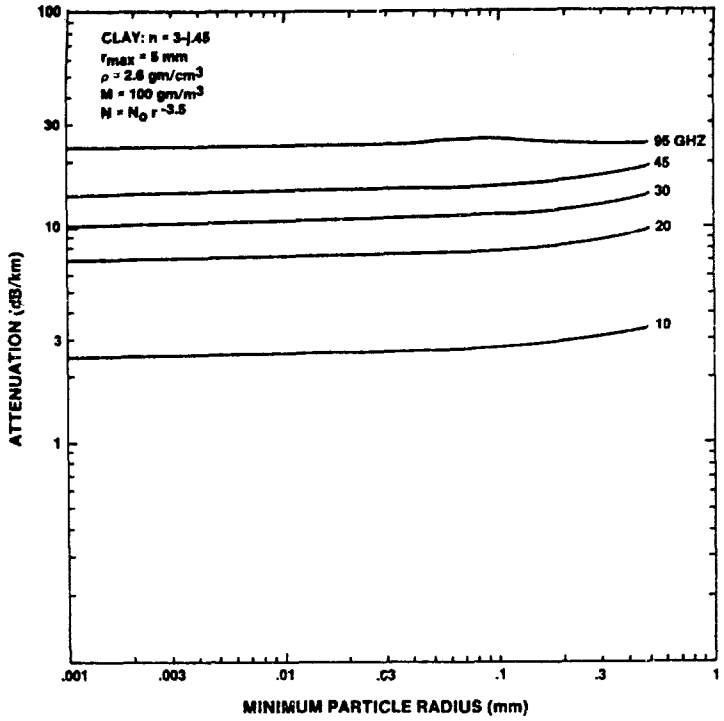

Figure 2b. Attenuation at Millimeter Wavelengths as a Function of Minimum Particle Radius, Clay

3.2 Dependence of Dust Attenuation and Albedo on Maximum Particle Radius

In Figures 3a and 3b, the attenuations and albedos are plotted for sand and clay respectively as a function of maximum particle radius for the same set of frequencies from 10 to 95 GHz. It is seen that the attenuation and albedo both rise very abruptly as the maximum particle radius is increased. The attenuation reaches a peak and the albedo begins to level off when the maximum particle diameter is approximately equal to the wavelength. As mentioned previously it is seen that the scattering losses are comparable and in some instances even larger than the absorption losses. This is due to the fact that the imaginary component of the index of refraction is very small, thus resulting in a small absorption.

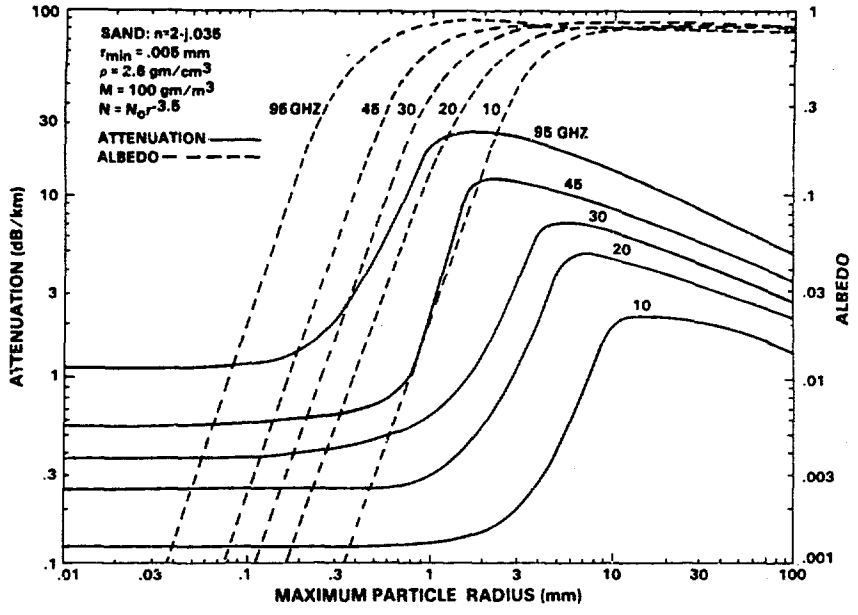

Figure 3a. Attenuation and Albedo at Millimeter Wavelengths as a Function of Maximum Particle Radius, Sand

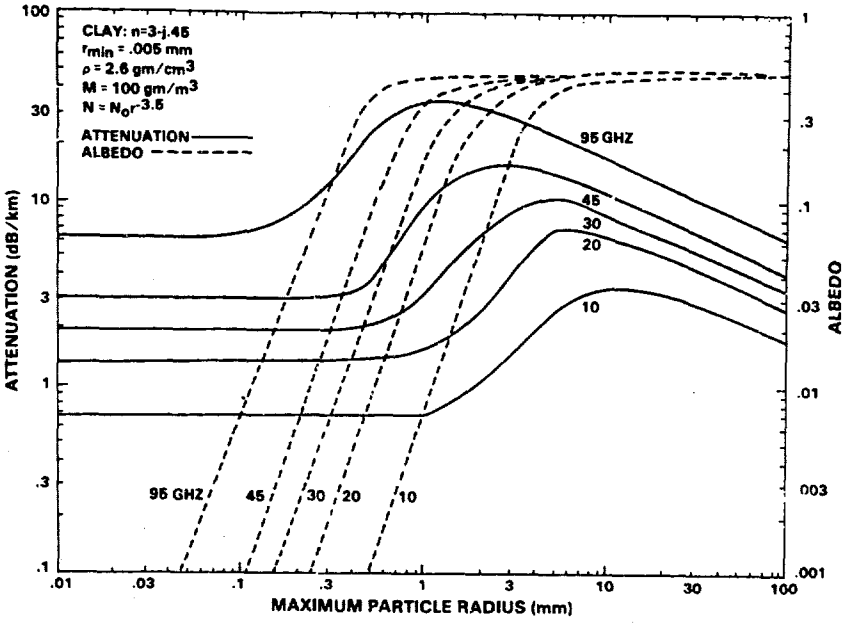

Figure 3b. Attenuation and Albedo at Millimeter Wavelengths as a Function of Maximum Particle Radius, Clay

3.3 Dependence of Dust Attenuation on the Power Law Exponent

In Figures 4a and 4b, attenuation is plotted as a function of power law exponent for sand and clay respectively for the set of frequencies from 10 to 95 GHz. When the exponent p, is small the probability of having large particles in the distribution is relatively high. As p becomes larger fewer large particles are present. Thus the attenuation passes through a very broad peak for low values of p and then drops off very rapidly when p becomes larger. Thus the power law exponent can significantly affect the attenuation.

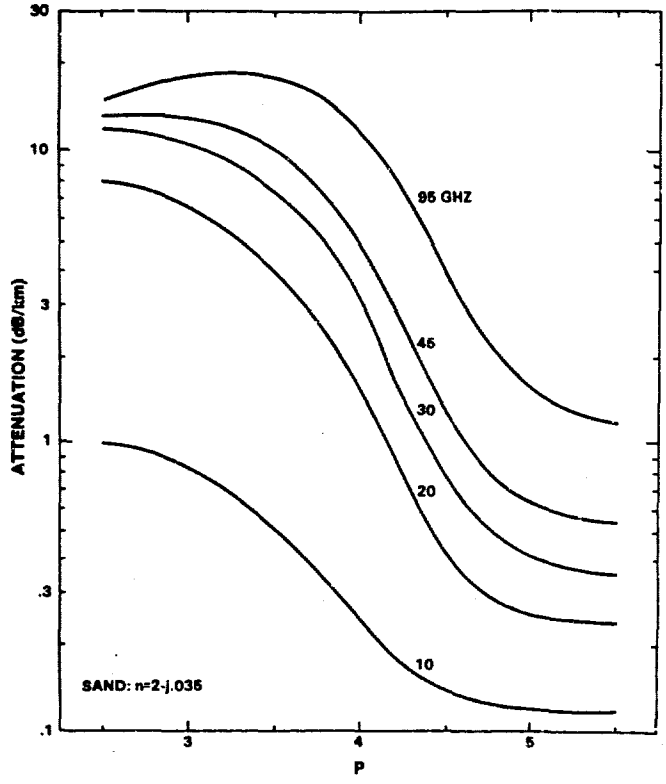

Figure 4a. Attenuation at Millimeter Wavelengths as a Function of Power Law Exponent, Sand

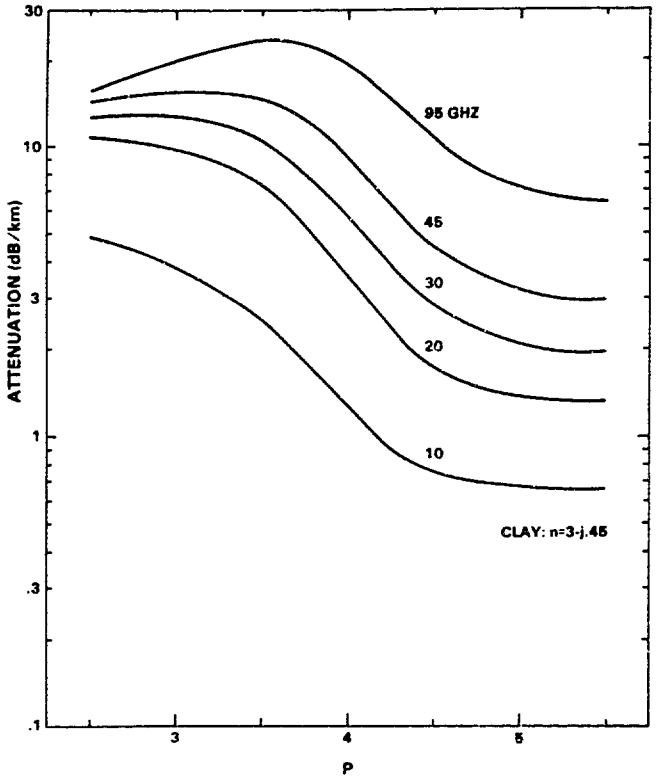

Figure 4b. Attenuation at Millimeter Wavelengths as a Function of Power Law Exponent, Clay

3.4 Dependence of Dust Attenuation and Albedo on the Index of Refraction

In Figure 5, the attenuation and albedo are plotted as a function of index of refraction $n = n_1 - jn_2$, for the set of frequencies from 10 to 95 GHz. Both the real and imaginary components of the index of refraction are increased linearly so that the particulates have an index of refraction that corresponds to dry sand for the lowest values and water for the highest values. It is seen that the attenuation increases and the albedo decreases sharply as the particulates change from dry sand to clay and then both essentially level off as the real and imaginary components are increased further. The attenuation and albedo are examined more closely in Figure 6. In Figure 6a, the imaginary component is fixed at $n_2 = 0.2$ and the real component is varied from 1.6 to 3.4; in Figure 6b, the real component is fixed at $n_1 = 2.5$, and the imaginary component is varied from zero to 0.6. For both cases the attenuation increases gradually as either of the components of index of refraction is increased. Based on the curves for the albedo it is seen that

increasing the imaginary component, increases the absorptive losses while increasing the real component results in an increase in the scattering losses. Thus it can be concluded that the attenuation is very dependent on both the real and imaginary components of the index of refraction over the ranges from about $2 < n_1 < 4$ and $0 < n_2 < \cdot\ 8$.

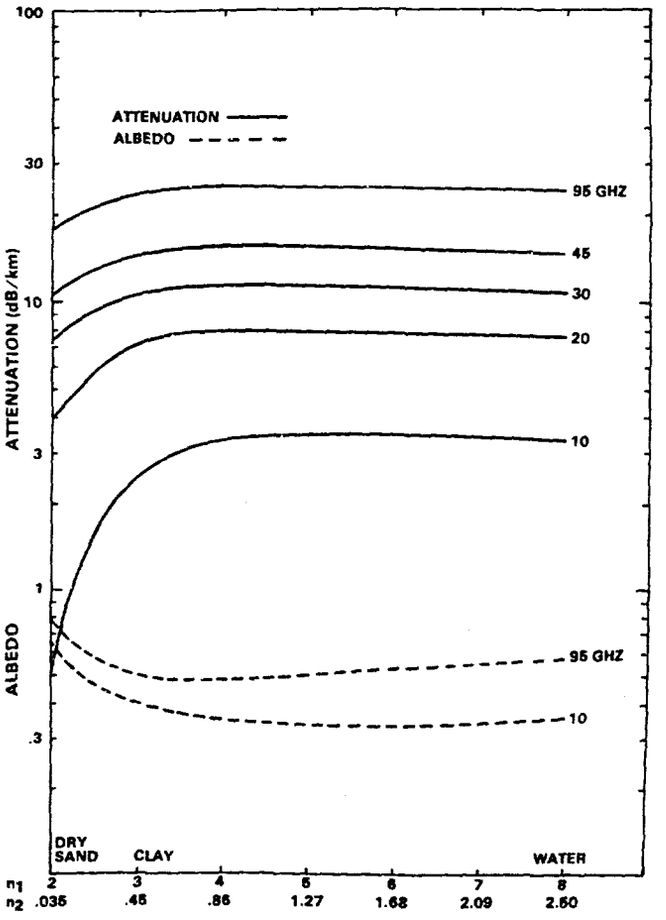

Figure 5. Attenuation and Albedo at Millimeter Wavelengths as a Function of Index of Refraction

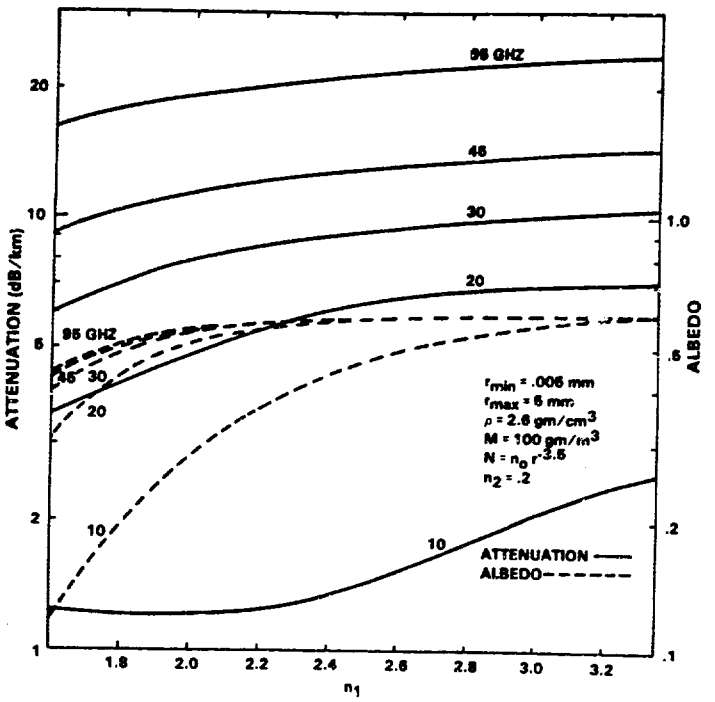

Figure 6a. Attenuation and Albedo at Millimeter Wavelengths as a Function of Real and Imaginary Components of Index of Refraction, Real Component

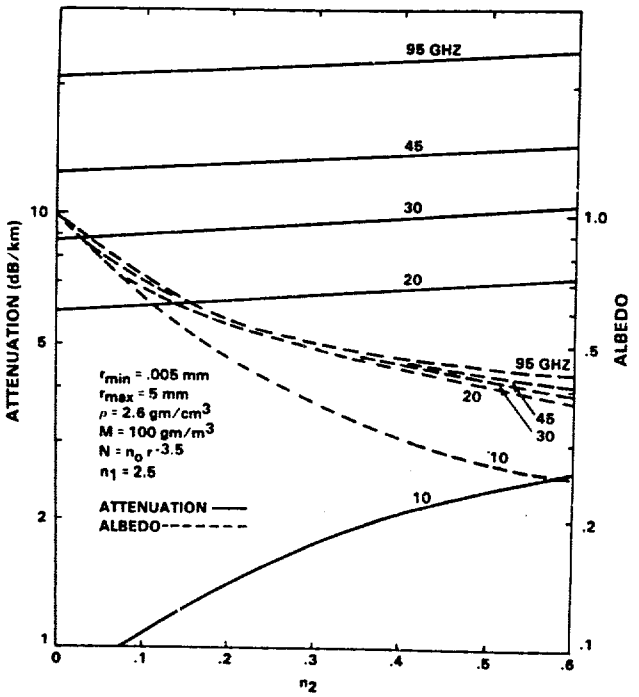

Figure 6b. Attenuation and Albedo at Millimeter Wavelengths as a Function of Real and Imaginary Components of Index of Refraction, Imaginary Component

3.5 Dependence of Dust Attenuation on Density of Particles

In Eq. (5) it is seen that the total number of dust particles is directly proportional to the total mass of the particles M_T, divided by the bulk density ρ_b of the individual particles. In this formulation a single scattering model is used so the attenuation is directly proportional to the number of particles as seen in Eq. (12) and therefore directly proportional to M_T/ρ_b. Thus any uncertainty in either the total mass or particle density will produce a corresponding error in the attenuation.

4. ATTENUATION PRODUCED BY A NUCLEAR BURST

As mentioned previously associated with the nuclear burst is a fireball. The initial electron density within the fireball is extremely high and for a period of about 20 sec blacks out the propagated wave. After that time, beta radiation from the radioactive debris within the fireball may sustain sufficiently high ionization levels to absorb millimeter wave signals for several minutes. Thus the two principal sources that attenuate the propagated wave are fireball ionization and dust.

The nuclear explosion dust model is often divided into five distinct regions which are modeled somewhat crudely in Figure 7. The ejecta region consists of relatively large particles of dust and debris thrown out of the crater; settling occurs quickly and its importance diminishes in about a minute or so. The blast wave produces a low level dust region often referred to as the pedestal or sweep-up layer. This region has high dust densities for about a minute also; lower densities exist for many minutes later. The cylindrical stem region forms after the establishment of the fireball vortex and lasts for several minutes. The mushroom shaped cloud or main cloud is the major dust region and exists for many minutes. Finally, the main cloud transcends into the fallout region which exists for a long period of time.

In this study the Weapons Effects on Satellite Communications code (WESCOM) is used. It utliizes environment, propagation and signal processing models developed by the Defense Nuclear Agency (DNA) and attempts to provide a best estimate of the quantities being modeled. Included along with ionization and dust losses are the oxygen and water vapor losses of the ambient troposphere.

The WESCOM dust model is a somewhat simplified model in that it assumes that all the dust is initially contained within the fireball and then forms a main cloud which eventually becomes the fallout region.[3] The stem and pedestal are not included in the WESCOM dust model. Dust particulates within the fireball are divided into the eight particle size ranges shown in Table 1.

---

3. Thompson, . . (1980) Dust Clouds - Models and Propagation Effects, Proceedings of Submillimeter Atmospheric Propagation Applicable to Radar and Missile Systems, Redstone Arsenal, Alabama, TR-80-3, pp. 114-117.

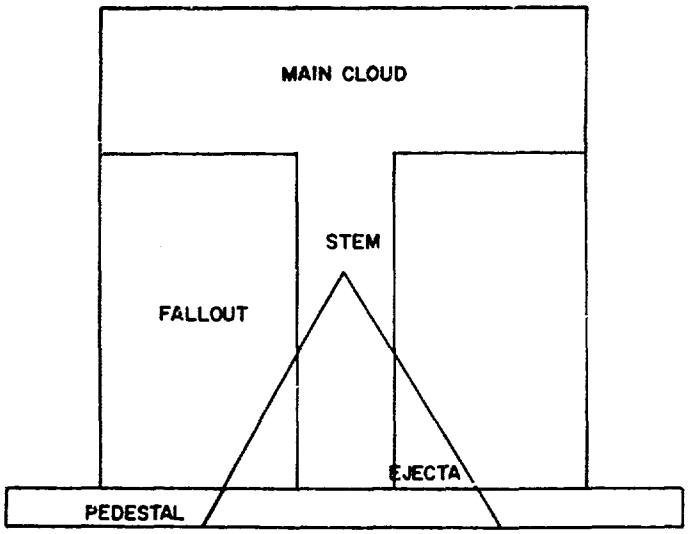

Figure 7. Dust Regions

Table 1. Particle Size Distribution

Dust Group	Minimum Particle Diameter	Fraction of Particles
1	0.0i mm	$1\text{-}1.372 \times 10^{-6}$
2	0.9	1.356×10^{-6}
3	4.0	1.463×10^{-8}
4	10.0	8.750×10^{-10}
5	20.0	9.587×10^{-11}
6	32.5	2.222×10^{-11}
7	52.5	4.540×10^{-12}
8	75	1.370×10^{-12}

Each group of particle sizes are initially assumed to be uniformly distributed throughout a disc-like cylinder. These discs are stacked within the fireball as shown in Figure 8a with the largest particles contained within the lowest disc and with decreasingly smaller particles in the upper discs. Each particle size group rises to a maximum altitude at which point the particles start to fall with their

respective terminal velocities. A simplified model of the size and height of the rising fireball as a function of time is shown in Figure 8b. The terminal velocities are plotted in Figure 9. Thus we have a model for which the largest particles remain aloft for a relatively short period of time while the smaller particles may remain suspended for many minutes.

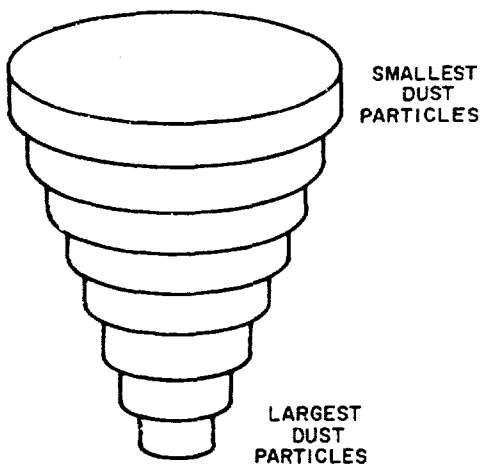

Figure 8a. Dust Model, Disc-like Regions Within Fireball

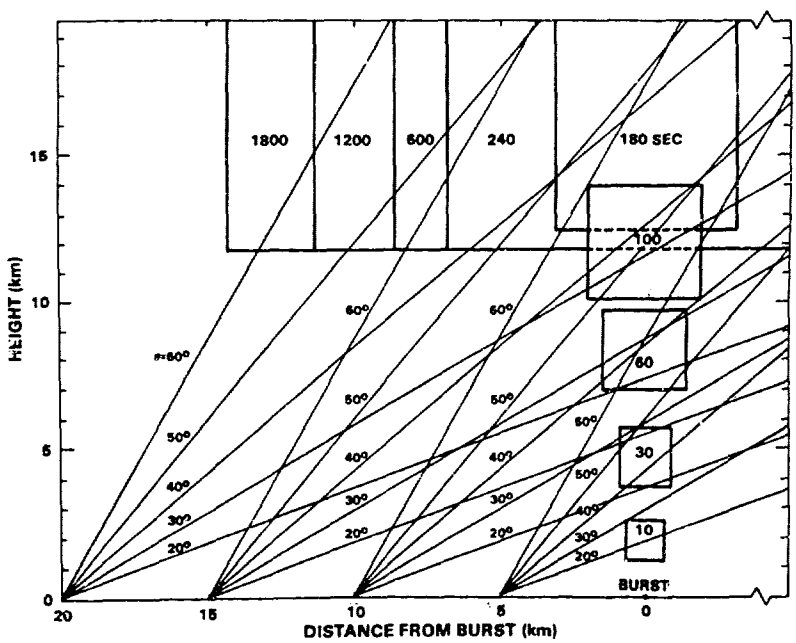

Figure 8b. Dust Model, Rising Fireball as a Function of Time

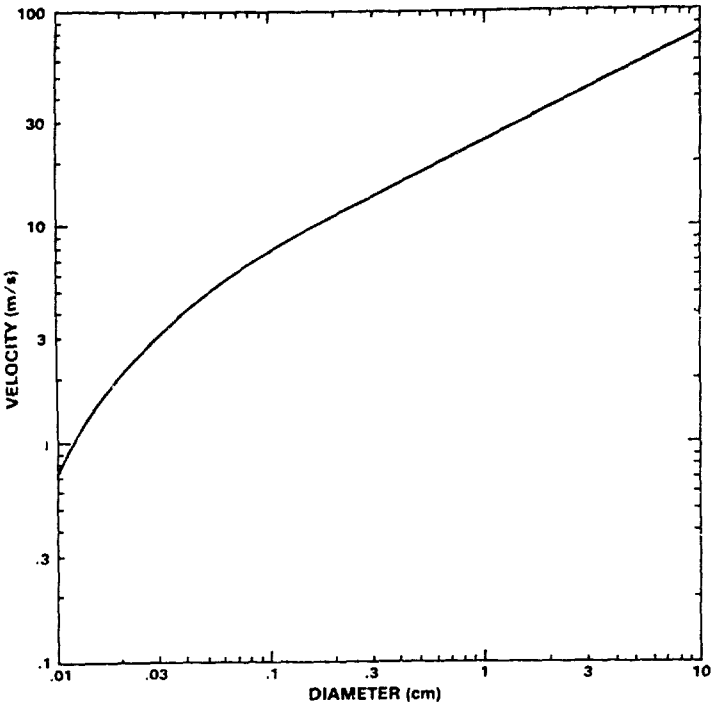

Figure 9. Terminal Velocity of Dust as a Function of Particle Radius

A set of attenuations were computed, using the WESCOM code, as a function of frequency, elevation angle, distance from the burst and time after burst for a megaton surface burst. In Figure 10 the attenuation is plotted as a function of time for a slant path 30° above the horizon, distance from burst of 10 km and frequencies of 10, 20, 45 and 95 GHz. It is seen that the attenuation has essentially two peaks; the first peak occurs about 35 sec after the burst and is caused by the dust rising through the antenna beam, the broader and lower attenuation second peak is due to the settling dust passing through the beam again. As expected, dust attenuation increases significantly with frequency.

In Figure 11 the angle dependence of the attenuation is examined for the same conditions at a frequency of 45 GHz. As expected the first peak occurs earliest and the attenuation is highest for the lowest elevation angle. Also the separation in time of the peaks decreases with increasing elevation angle.

In Figure 12 the distance dependence of the attenuation is plotted for the same conditions for a fixed elevation angle of 30°. It is seen that the highest attenuations occur earliest for distances closest to the burst and then decrease and occur at later times as the distance from the burst is increased.

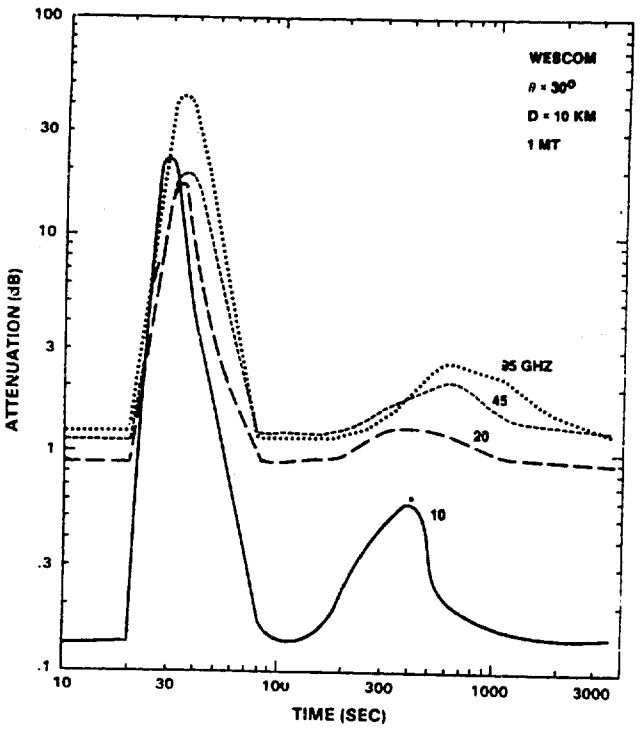

Figure 10. Attenuation From 1 MT Burst as a Function of Frequency

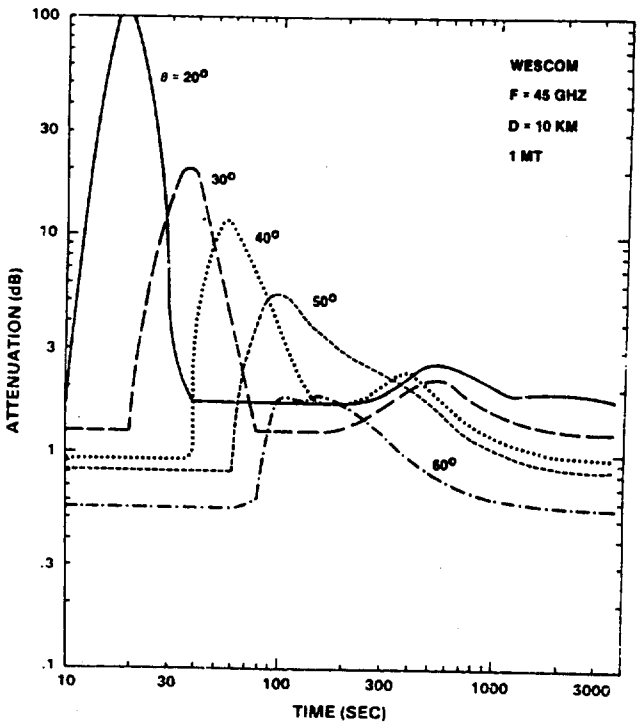

Figure 11. Attenuation From 1 MT Burst as a Function of Elevation Angle

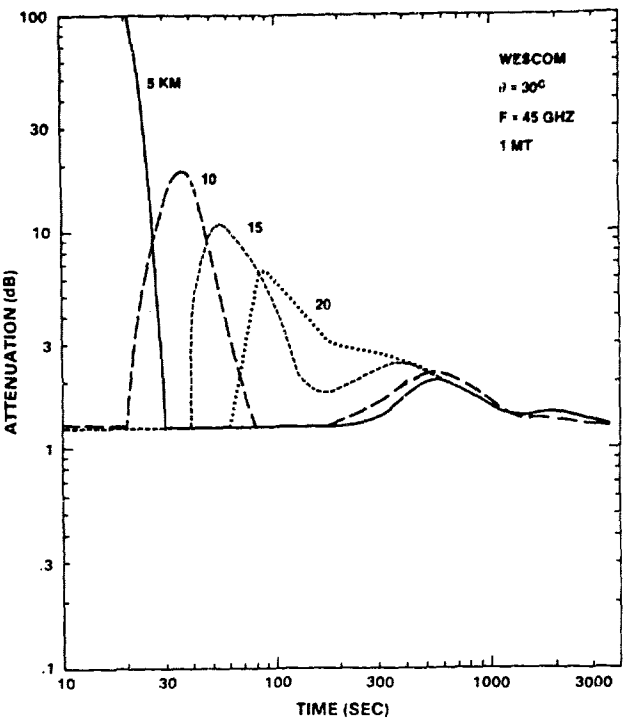

Figure 12. Attenuation From 1 MT Burst as a Function of Distance From Burst

In general it is seen that high attenuations occur at all frequencies as the rising dust cloud passes through the antenna beam. For low elevation angles and distances close to the burst these attenuations may exceed 100 dB. Attenuations produced by the falling dust are significantly lower and do not generally exceed 5 dB.

5. CONCLUSIONS

Upon examining the effects of dust on slant path propagation at millimeter wavelengths it has been shown that the attenuation is heavily dependent on the maximum particle radius, the number of large particles in the distribution and the real and imaginary components of the index of refraction in the range from dry sand to clay. The attenuation is also directly proportional to the fraction of the atmosphere filled with dust. Dust attenuations, while low at frequencies below 10 GHz increase significantly at millimeter wavelengths.

For the WESCOM code, the computed attenuations behave as would be expected. Very large attenuations occur immediately after the burst due to fireball ionization

and dust when the antenna beam is close to the fireball. At later times the attenuation is caused mostly by dust. The attenuation due to oxygen and water vapor is typically less than 1 dB in the window region.

On the basis of these results it appears that if the antenna beam intersects the fireball within the first 20 sec after the burst, then attenuations greater than 100 dB are likely, and the lower frequencies are attenuated more than the higher frequencies because the losses are due predominantly to fireball ionization. For this reason it would seem that the very early dust model is not too critical since the attenuations are always prohibitive. At times from about 20 sec to several minutes, the period after ionization losses have essentially disappeared, but during which dust losses can be tens of dB's, the accuracy of the dust model parameters discussed above can significantly influence the results. Finally, when the dust settles, although attenuations of the order of several dB are likely, it would seem that it should be possible to model these more accurately than those at earlier times since the terminal velocities of the dust particles are known. Since only the very small particles remain suspended the size distribution is less critical and only the density and index of refraction of the dust are important.

MISSION
of
Rome Air Development Center

RADC plans and executes research, development, test and selected acquisition programs in support of Command, Control, Communications and Intelligence (C^3I) activities. Technical and engineering support within areas of competence is provided to ESD Program Offices (POs) and other ESD elements to perform effective acquisition of C^3I systems. The areas of technical competence include communications, command and control, battle management, information processing, surveillance sensors, intelligence data collection and handling, solid state sciences, electromagnetics, and propagation, and electronic, maintainability, and compatibility.

Printed by
United States Air Force
Hanscom AFB, Mass. 01731